Experiment on Leader Propagation Characteristics of Air Gaps in UHVDC Transmission Towers Under Positive Switching Impulse Voltages

Xuan Zhou, She Chen, Hai Wang, Rong Zeng, *Senior Member, IEEE*, Chijie Zhuang, *Member, IEEE*, Junjie Yu, and Yujian Ding

***Abstract*—Rapid developments in EHV/UHV transmission systems require a deeper understanding of the mechanism of long air gap discharge. Leader propagation is one of the main processes in long gap breakdown. In this paper, the leader propagation characteristics of real size ±800 kV UHVDC transmission tower gaps under positive switching impulse voltages (185/ 2290 μs) are investigated. An integrated observation platform consisting of an impulse voltage divider, a coaxial shunt, a high-speed video camera, and a set of integrated optical electric field sensors (IOES), is established. The waveforms of impulse voltage, discharge current, electric field variation at specific positions, and time-resolved photographs of discharge morphology are recorded. Axial leader velocity and the relationship between leader advancements and injected charge are obtained. The typical value of leader stable propagation velocity is 1.7–2.2 cm/μs, which varies slightly with the gap length and applied voltage amplitude. The leader velocity in the re-illumination process is much higher, and is seen as varying from 5 cm/μs to 30 cm/μs, with an average value around 10 cm/μs. The charge in leader channel per unit length is 20–40 μC/m, which illustrates a near-direct proportion relationship between discharge current and leader velocity. The observed parameters are important for further simulation of the tower gap breakdown processes.**

***Index Terms*—Integrated observation platform, leader propagation characteristics, long air gap discharge, positive switching impulses, UHVDC transmission tower.**

I. Introduction

THE demand for electric power in China is increasing rapidly. Because the energy bases are far away from the load centers, massive long distance transmission systems with large capability have been constructed. Three 1000 kV UHVAC transmission projects and four ± 800 kV UHVDC transmission projects have become operational since 2014. An important issue in EHV/UHV transmission systems is to determine external insulation distances, which requires extensive knowledge of the mechanism and characteristics of long air gap discharge [1]–[4]. A number of experiments have been carried out to obtain the breakdown characteristics of some typical engineering gaps. Transmission tower gaps are one of the most common engineering gaps, for which the influences of gap length, gap structure, voltage shape and polarity, altitude on the 50% breakdown voltage U_{50}— all have been investigated through simulation experiments. However, the physical processes and parameters of discharge propagation on tower gaps have been rarely studied [5]–[8].

Leader propagation is one of the main processes in long air discharge. Parameters such as leader velocity and charge in leader channel per unit length are important in the simulation of long gap breakdown [9]–[13], and laboratory experiments have been conducted to study leader propagation in rod-rod or rod-plane gaps. The most common method applied for observing leader propagation is streak photography using image converter cameras (ICC) [14]–[20]. The famous research conducted by Les Renardières Group in the 1970s using ICC and still cameras provides extensive information on positive leader discharges in gaps with lengths up to 10 m under switching impulse voltages [14]–[16]. The typical leader velocity is 1.25–3 cm/μs, and the charge in leader channel per unit length is 20–60 μC/m, which varies with electrode configuration, applied impulse shape, and environmental conditions.

In recent years, advancements in observation and measurement techniques provide new approaches for investigating long air gap discharges [21]–[23]. One of the most outstanding techniques is high-speed photography using CMOS (complementary metal oxide semiconductor) or CCD (charge-coupled device) video cameras, which permit us to obtain clear discharge luminous morphology, especially the leader channels with relatively weak luminosity, which are usually not distinct in streak images. The discharge in typical gaps has been observed with high time-resolution (in orders of microseconds or even nanoseconds) using high-speed CMOS/CCD cameras, and parameters such as leader velocity have also been derived [24]–[29]. Another important technique is the integrated optical electric field sensor (IOES) based on Pockels effect, which has been used for obtaining the electric field and its variations, including discharges at specific positions, thus

Manuscript received May 11, 2015; revised August 17, 2015; accepted August 19, 2015. Date of publication September 30, 2015; date of current version September 9, 2015. This work was supported by the National Natural Science Foundation of China under Grant 51325703, 51377094 and Fund of the National Priority Basic Research of China (2011CB209403).

X. Zhou, H. Wang, R. Zeng, C. Zhuang, and J. Yu are with the Department of Electrical Engineering, State Key Lab of Power System, Tsinghua University, Beijing 100084, China (e-mail: zhouxuan12@ mails.thu.edu.cn; wangh0117@yeah.net; zengrong@thu.edu.cn; chijie@thu.edu.cn; dajiaoyu0401@163.com).

S. Chen is with the College of Electrical and Information Engineering, Hunan University, Changsha 410082, China (e-mail: chenshethu@gmail.com).

Y. Ding is with China Electric Power Research Institute, Beijing 100192, China (e-mail: dingyj@epri.sgcc.com.cn).

Digital Object Identifier 10.17775/CSEEJPES.2015.00034

providing information on the production and propagation of space charge [30]–[33].

In this paper, an integrated observation platform containing measurements of current, voltage, electric field, and high-speed photography is established to investigate positive leader propagation characteristics in real size UHVDC transmission tower gaps. The discharge current, electric field variation, and time resolved images of air gap breakdown processes are obtained, and leader velocity and charge per unit length under switching impulse voltages are derived, offering important parameters for simulation of tower gap breakdown.

II. Experimental Details

A. Integrated Observation Platform

The integrated observation platform established in the experiments and described in this paper consists of an impulse divider to record the applied voltage waveforms, a coaxial shunt to record the discharge current, a set of IOESs to detect the electric field E at specific positions, and a CMOS high-speed video camera. The schematic diagram of the platform is shown in Fig. 1.

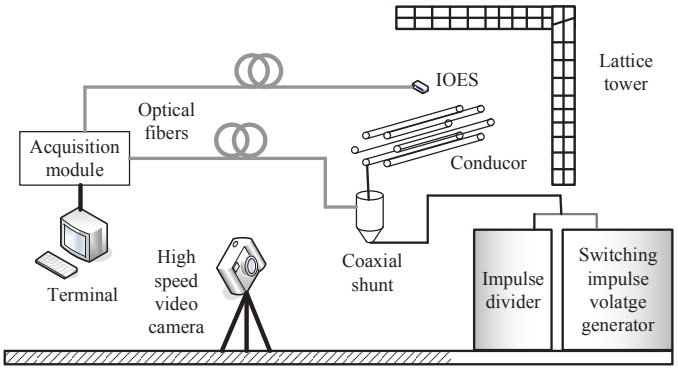

Fig. 1. Schematic diagram of the integrated observation platform for switching impulse discharge in tower head gaps.

The experimental set up was as follows: The coaxial shunt was placed in a shielding barrel and connected to the conductor and high voltage lead. Data from the current was sampled by a data acquisition card (NI USB-5133) and transmitted through optical fibers. Three IOESs were used in this platform. The principle and typical applications of the sensors are presented in [31]–[33]. The high-speed camera (Phantom V12.1) has a maximum frame rate of 680, 000 fps (frames per second) with an image size of 128 $\times$ 8 pixels. To achieve a considerable time-space resolution, the camera was operated at a frame rate of 120, 171 fps (8.32 μs interval) with an exposure time of 7.68 μs each frame, and the corresponding image size is 256 $\times$ 128 pixels.

B. Experimental Arrangements

The arrangements of the real-size simulation tower head gaps are shown in Fig. 2. Two typical arrangements were followed in this experiment: 1) The minimum distances between the corona rings to the cross arm (L_1) and the lateral column (L_2) of tower were set to approximately 6.1 m. 2) L_1 and L_2 of tower were set to approximately 8.45 m. The simulation conductor used in the experiments was 6-bundled, and 25 m in length and 17 m in height from the ground. The external radius of the corona rings was 1120 mm and the pipe diameter was 120 mm. All the components were assembled based on the requirements for $\pm$ 800 kV UHVDC projects. The three IOESs were aligned between the corona rings and the cross arm, as shown in Fig. 2. Fig. 3 is a photograph of the testing site. The structure of the tower gap and the arrangements of the IOESs and coaxial shunt can be clearly recognized in the photo.

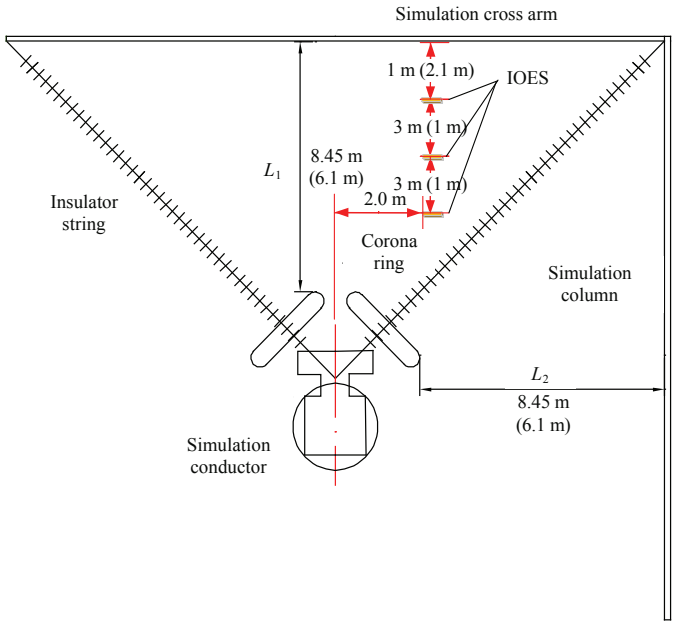

Fig. 2. Schematic diagram of the configuration of testing gaps and arrangements of IOES.

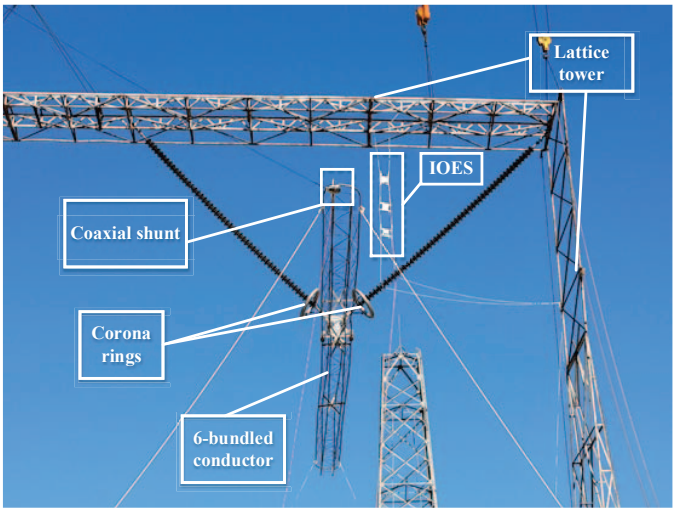

Fig. 3. Photograph of the experimental arrangements.

C. Testing Conditions

Positive switching impulse voltages (185/2290 μs) generated by a 7.2 MV Marx generator were applied to the

conductor. The parameters of testing conditions are shown in Table I. In the experiments, the temperature was 23–28°C and the relative humidity was 46%–77%. Breakdown occurred to the cross arm or the lateral column randomly. In the following analysis, only the cases of cross arm breakdown are considered.

TABLE I
PARAMETERS OF TESTING CONDITIONS

No.	L_1 (m)	L_2 (m)	U_{cr}^a (kV)
1	6.10	6.10	1,888
2	6.10	6.10	2,231
3	8.45	8.45	2,231
4	8.45	8.45	2,746

[a] U_{cr} is the crest value of the switching impulse voltage.

III. TYPICAL RECORDING

A. Waveforms of Voltage and Current

A typical recording of current and voltage waveforms is shown in Fig. 4. In this example, the voltage amplitude was 1888 kV, and the gap length L_1 was 6.1 m. The total current consists of two parts: the capacitive current and the discharge current (conduction current). The capacitive current can be derived from the derivative of voltage; thus the discharge current can be obtained by subtracting the capacitive current from the total current. The discharge was initiated at approximately 50 μs and breakdown occurred at approximately 200 μs. It is difficult, however, to determine the continuous leader inception time only from the current waveform.

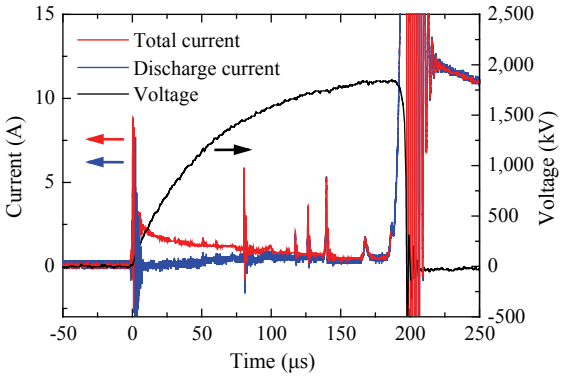

Fig. 4. Typical waveforms of discharge current and impulse voltage ($L_1 = L_2 = 6.1$ m, $U_{cr} = 1888$ kV).

B. High-Speed Photography

The background photograph and time-resolved images of discharge luminous morphology are shown in Fig. 5. The continuous leader inception time can be obtained from discharge current shown in Fig. 4 and from the morphology images. A few unstable leaders initiated around 80 μs and extinguished after short periods; the continuous leader initiated at 113 μs from the corona ring. The luminous intensity of leader channel in images (11), (15), and (17) was apparently stronger than in other images before breakdown. This phenomenon is known as re-illumination (or restrike), and the corresponding large current impulse can be observed in Fig. 3.

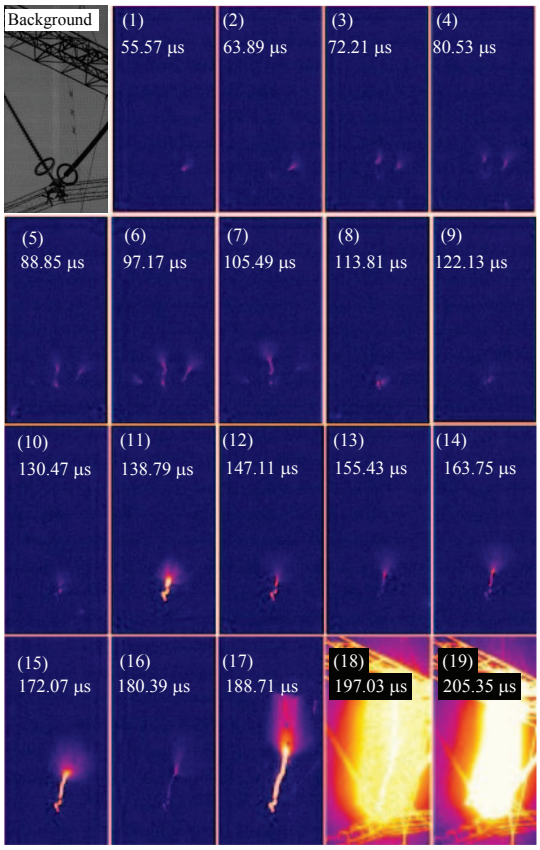

Fig. 5. Typical time-resolved images of discharge luminous morphology, taken by high-speed video camera with a frame interval of 8.32 μs ($L_1 = L_2 = 6.1$ m, $U_{cr} = 1888$ kV).

The leader length and leader velocity as functions of time can be derived from the time-resolved images. In this paper, the axial leader length l_z and axial leader velocity v_{lz} are considered (the axial direction here is perpendicular to the cross arm). The temporal variation of l_z and v_{lz} of this example is shown in Fig. 6. The stable velocity of leader propagation was around 2 cm/μs and the velocity during re-illumination was larger than 5 cm/μs. The velocity of final jump was no less than 33 cm/μs due to the limitation in time resolution.

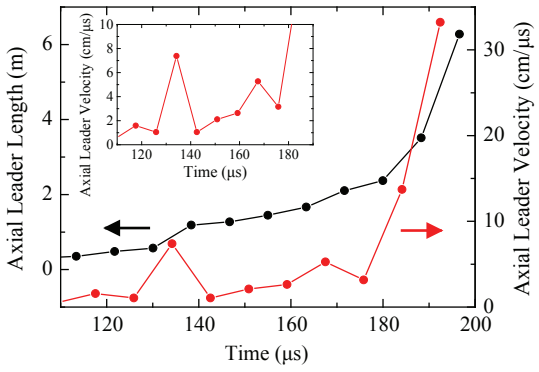

Fig. 6. The temporal variation of leader axial length and velocity ($L_1 = L_2 = 6.1$ m, $U_{cr} = 1888$ kV).

C. Waveforms of Electric Field

The waveforms of electric field E at three specific positions are shown in Fig. 7. The bottom IOES was the nearest the 6-bundled conductor while the top one was the nearest to the cross arm. Electric field step increments can be observed in the waveforms, as arrows and dash lines in Fig. 7, which were caused by the rapid production of space charge. With the leader-streamer propagation, the electric field at the positions behind the streamer zone stopped rising and remained at a relatively stable value before the final jump and gap breakdown. Thus, there was only one field step detected by the bottom IOES and two steps detected by the middle one. As the electric fields stopped rising at different positions, the propagation velocity of space charge region (the leader-streamer system) v_{q} can be estimated. The velocity v_{q} at 145–170 μs was about 4 cm/μs, and at 170–190 μs was about 5 cm/μs. The value of v_{q} was similar to the leader propagation velocity v_{lz} obtained from the high-speed images. This indicates that the electric field measurements provide an auxiliary approach for evaluating the propagation velocity of discharge. Since the domain of streamer region and the distribution of space charge typically change with discharge development, there could be some difference between v_{q} and v_{lz}.

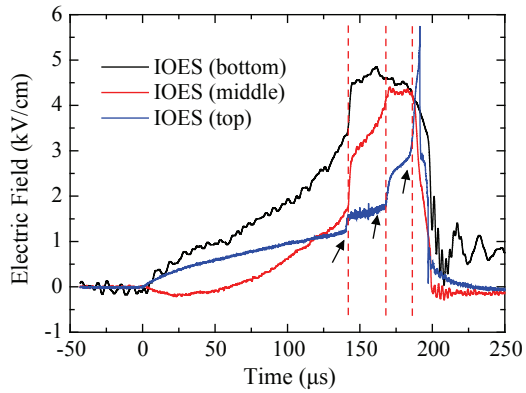

Fig. 7. Typical waveforms of electric field at specific positions ($L_1 = L_2 = 6.1$ m, $U_{\mathrm{cr}} = 1888$ kV).

IV. Results and Discussion

A. Leader Length and Velocity

The temporal variation of axial leader length was measured from the high-speed images. Fig. 8 shows the results obtained from the experiments for the 6.1 m tower gap with 2231 kV switching impulse voltages. The leader length before final jump was about 3.2 m and the final jump length L_{f} was about 3 m.

The axial leader velocity was derived from the advancements of leader length versus time, as shown in Fig. 9. In this condition, the velocity of leader stable propagation v_{s} was usually lower than 5 cm/μs with an average value of 1.88 cm/μs. When the re-illumination process occurred, the leader velocity v_{r} was much higher, varying from 5 cm/μs to 30 cm/μs. In the final jump stage, the velocity was higher than 30 cm/μs.

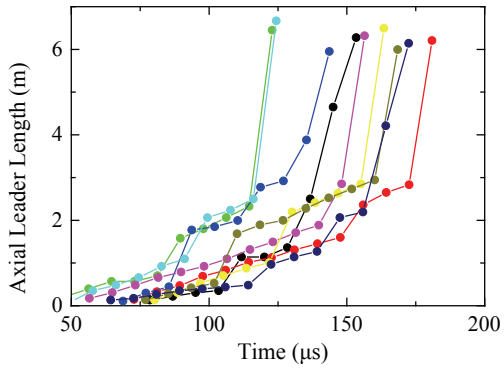

Fig. 8. Axial leader length as function of time ($L_1 = L_2 = 6.1$ m, $U_{\mathrm{cr}} = 2231$ kV).

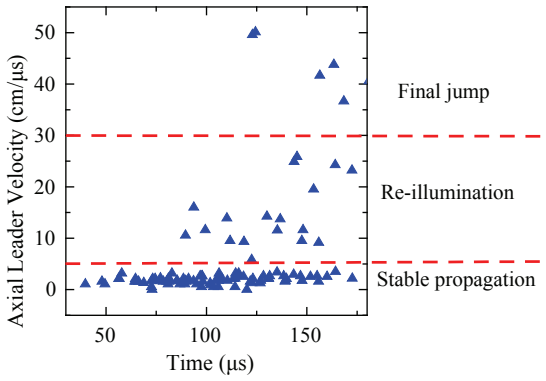

Fig. 9. Axial leader velocity as function of time ($L_1 = L_2 = 6.1$ m, $U_{\mathrm{cr}} = 2231$ kV).

The average values of v_{s} and v_{r} in different testing conditions are given in Table II. The average stable propagation velocity v_{s} is 1.7–2.2 cm/μs, and the average value of leader velocity v_{r} during re-illumination is around 10 cm/μs. Leader propagation velocity is mainly related to the electric field and ambient humidity. The stable propagation velocities v_{s} in the four conditions are very close, slightly increasing with gap length and applied voltage amplitude. It is easy to understand that with higher applied voltage, the geometric electric field in the gap is correspondingly higher, resulting in higher leader velocity. For testing conditions 2 and 3, the applied voltages are the same. The experiments show that the duration of leader propagation in the 8.45 m gap is longer than the 6.1 m gap, especially for the period close to the crest of the applied voltage. Moreover, the non-uniformity of electric field in the 8.45 m gap is larger. This indicates that the electric field in front of the leader tip is higher in the 8.45 m gap, which

TABLE II
Average Values of Final Jump Length, Axial Leader Velocity, and Leader Charge Per Unit Length in Different Testing Conditions

L_1 (m)	U_{cr} (kV)	L_{f} (m)	v_{s} (cm/μs)	v_{r} (cm/μs)	q_{lz} (μC/m)
6.10	1,888	3.24	1.75	9.93	24.98
6.10	2,231	3.05	1.88	14.68	32.13
8.45	2,231	2.94	1.96	11.82	21.84
8.45	2,746	3.99	2.11	11.35	31.43

results in higher leader velocity. As to the ambient humidity, it has obvious influences on the probability of re-illuminations, which is generally observed during the leader propagation process with high ambient humidity.

B. Relationship Between Leader Advancements and Injected Charge

The relationship between axial leader velocity $v_{\rm lz}$ and the current flowing through the leader tip I can be expressed as (1) [9]–[11],

$$v_{\rm lz} = I/q_{\rm lz} \tag{1}$$

where $q_{\rm lz}$ is the charge in leader channel per unit axial length.

An example of the relationship between leader propagation and injected charge is shown in Fig. 10. The results were obtained from experiments for the 8.45 m tower gap with 2746 kV switching impulse voltages. In Fig 10, the horizontal coordinate represents the axial leader length minus the initial value obtained from the first photograph showing continuous leader propagation. The vertical coordinate represents the total injected charge after the end moment of the first photograph of continuous leader. The axial leader length was approximately proportional to the inject charge after leader inception, and then $q_{\rm lz}$ can be derived. In this testing condition, $q_{\rm lz}$ was estimated to be 31.43 μC/m. The values of $q_{\rm lz}$ in other testing conditions are given in Table II, varying from 20 to 40 μC/m. Note that the current measured by the coaxial shunt is not exactly the current flowing through the continuous leader tip, because there would be several coronas or leaders developed from other positions along the testing conductor. As Fig. 5 shows, there was almost no obvious discharge except for the main leader-streamer system after the continuous leader initiated. The current waveform shown in Fig. 4 has good correspondence with the leader propagation process. Thus, we simplified the calculation of injected charge without taking into account the charge produced by other coronas or leaders. It would make the obtained values of charge per leader length larger than the actual ones.

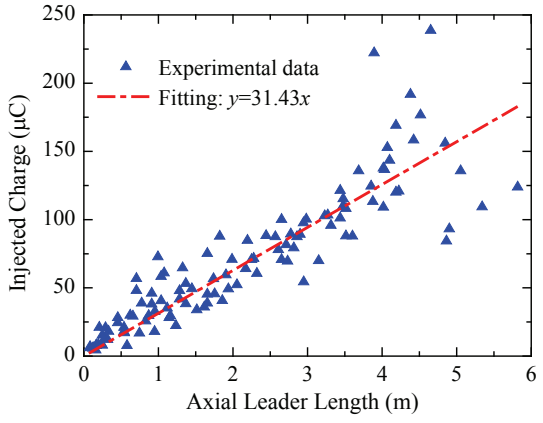

Fig. 10. Relationship between axial leader length and injected charge ($L_1 = L_2 = 8.45$ m, $U_{\rm cr} = 2746$ kV).

V. Conclusions

An integrated observation platform was established to investigate the leader propagation characteristics of real-size simulation tower gaps in UHVDC transmission projects. The minimum distance from corona rings and tower lattice was arranged to be 6.1 m and 8.45 m. Positive switching impulse voltages (185/2290 μs) were applied to the gaps. Waveforms of applied impulse voltage, discharge current, space electric, and high-speed photographs showing the luminous morphology of discharge, all were obtained.

Leader velocity was derived from time-resolved images. The average axial leader velocity of stable propagation varied from 1.7 to 2.2 cm/μs, increasing with gap length and applied voltage amplitude. The velocity during re-illumination was much higher with an average value around 10 cm/μs. In addition, the charge in leader channel per axial length was also estimated from the relationship between leader length and injected charge. The typical value varied from 20 to 40 μC/m. Leader velocity and the relationship between leader advancement and injected charge are important parameters in prediction of 50% breakdown voltages.

Acknowledgment

The authors would like to thank China Electric Power Research Institute for providing test site and staff. In addition, the authors would like to express grateful appreciation to Chanxiao Li, Gang Lv and Zhizhao Li for assisting in the experiments.

References

[1] China Electric Power Encyclopedia, *Power Transmission and Transformation*. Beijing, China: China Electric Power Press, 2014, pp. 30–32.
[2] Q. Yuan, "Present state and application prospect of ultra HVDC transmission in China," *Power System Technology*, vol. 29, no. 14, pp. 1–3, Jul. 2005.
[3] Y. Shu, Z. Liu, L. Gao, and S. Wang, "A preliminary exploration for design of ±800 kV UHVDC project with transmission capacity of 6400 MW," *Power System Technology*, vol. 30, no. 1, pp. 1–8, Jan. 2006.
[4] R. Zeng, C. Zhuang, Z. Yu, S. Chen, Z. Li, and W. Chen, "Challenges and achievement in long air gap discharge research," *High Voltage Engineering*, vol. 40, no. 10, pp. 2945–2955, Oct. 2014.
[5] W. Zhang, C. Gu, W. Liao, Y. Ding, and J. Fan, "Impulse voltage flashover characteristic of air gap in EHV/UHV DC transmission tower," *Proceedings of the CSEE*, vol. 30, no. 1, pp. 1–5, Jan. 2010.
[6] Y. Ding, W. Liao, Z. Su, Z. Zhang, and F. Lv, "Research on the influence factors of discharge characteristics of air gaps for ± 800 kV double line transmission towers," *Proceedings of the CSEE*, vol. 34, no. 18, pp. 2983–2989, Jan. 2014.
[7] Y. Ding, W. Liao, Z. Sun, and Z. Su, "Experimental studies on impulse flashover characteristics of tower head air gaps of ±1000 kV DC transmission lines and altitude correction methods," *Proceedings of the CSEE*, vol. 31, no. 34, pp. 156–162, Dec. 2011.
[8] C. Gu, W. Zhang, and J. Fan, "Summary of experimental study on switching impulse flashover characteristics of typical air gaps in EHV/UHV transmission systems," *Power System Technology*, vol. 35, no. 1, pp. 11–17, Jan. 2011.
[9] I. Gallimberti, "The mechanism of the long spark formation," *Journal de Physique Colloques*, vol. 40, no. C7, pp. 193–250, Jul. 1979.
[10] A. Bondiou and I. Gallimberti, "Theoretical modeling of the development of the positive spark in long gaps," *Journal of Physics D: Applied Physics*, vol. 27, no. 6, pp. 1252–1266, Jun. 1994.
[11] N. Goelian, P. Lalande, A. Bondiou, G. L. Bacchiega, A. Gazzani, and I. Gallimberti, "A simplified model for the simulation of positive-spark development in long air gaps," *Journal of Physics D: Applied Physics*, vol. 30, no. 17, pp. 2441–2452, Sep. 1997.

[12] I. Fofana and A. Beroual, "A new proposal for calculation of the leader velocity based on energy considerations," *Journal of Physics D: Applied Physics*, vol. 29, no. 3, pp. 691–696, Jun. 1996.

[13] M. Becerra and V. Cooray, "A self-consistent upward leader propagation model," *Journal of Physics D: Applied Physics*, vol. 39, no. 16, pp. 3708–3715, Aug. 2006

[14] Les Renardières Group, "Research on long air gap discharges at Les Renardières," *Electra*, no. 23, pp. 53–157, Jul. 1972.

[15] Les Renardières Group, "Research on long air gap discharges at Les Renardières-1973 results," *Electra*, no. 35, pp. 49–156, Jul. 1974.

[16] Les Renardières Group, "Positive discharges in long air gap discharges at Les Renardières-1975 results and conclusions," *Electra*, no. 53, pp. 31–153, Jun-Jul. 1977.

[17] Les Renardières Group, "Negative discharges in long air gap discharges at Les Renardières," *Electra*, no. 74, pp. 67–216, 1981.

[18] P. Domens, A. Gibert, J. Dupuy, and B. Hutzler. "Propagation of the positive streamer-leader system in a 16.7 m rod-plane gap," *Journal of Physics D: Applied Physics*, vol. 24, no. 10, pp. 1748–1757, Oct. 1991.

[19] P. Lalande, A. Bondiou, G. Bacchiega, and I. Gallimberti, "Observations and modeling of lightning leaders," *Comptes Rendus Physique*, vol. 3, no. 10, pp. 1375–1392, 2002.

[20] A. G. Andreev, E. M. Bazelyan, M. U. Bulatov, I. P. Kuzhekin, L. M. Makalsky, D. I. Sukharevskij, and V. S. Syssoev. "Experimental study of the positive leader velocity as a function of the current in the initial and final-jump phases of a spark discharge," *Plasma Physics Reports*, vol. 34, no. 7, pp. 609–615, Jul. 2008.

[21] R. Zeng, Y. Geng, B. Niu, Z. Yu, Z. Li, and F. Wang, "Research progress on parameters measurement of air gap discharge," *High Voltage Engineering*, vol. 37, no. 3, pp. 528–536, Mar. 2011.

[22] W. Chen, S. Gu, S. Xie, B. Sun, H. He, J. Chen, J. He, G. Qian, and N. Xiang, "Experimental observation technology for long air gap discharge," *Proceedings of the CSEE*, vol. 32, no. 10, pp. 13–21, Apr. 2012.

[23] S. Gu, J. Chen, W. Chen, Z. Ding, H. He, and G. Qian. "Establishment of integrated observation system for long air gap discharges," *High Voltage Engineering*, vol. 35, no. 11, pp. 2640–2646, Nov. 2009.

[24] Z. Li, R. Zeng, Z. Yu, S. Chen, Y. Liao, and R. Li, "Research on the upward leader emerging from transmission line by laboratory experiments," *Electric Power Systems Research*, vol. 94, pp. 64–70, Jan. 2013.

[25] R. Zeng, Z. Li, Z. Yu, C. Zhuang, and J. He, "Study on the influence of the DC voltage on the upward leader emerging from a transmission line," *IEEE Transactions on Power Delivery*, vol. 28, no. 3, pp. 1674–1681, Apr. 2013.

[26] Y. Geng, C. Zhuang, R. Zeng, Z. Li, and Z. Yu, "Leader development velocity based on leader channel three dimensional spatial structure," *High Voltage Engineering*, vol. 38, no. 9, pp. 2465–2472, Sep. 2012.

[27] S. Gu, W. Chen, J, Chen, H. He, and G. Qian, "Observation of the streamer-leader propagation processes of long air-gap positive discharges," *IEEE Transactions on Plasma Science*, vol. 38, no.2, pp. 214–217, Feb. 2010.

[28] R. Zeng and S. Chen, "The dynamic velocity of long positive streamers observed using a multi-frame ICCD camera in a 57 cm air gap," *Journal of Physics D: Applied Physics*, vol. 46, no. 48, pp. 485201-1–485201-10, Nov. 2013.

[29] S. Chen, R. Zeng, and C. Zhuang. "The diameters of long positive streamers in atmospheric air under lightning impulse voltage," *Journal of Physics D: Applied Physics*, vol. 46, no. 37, pp. 375203-1–375203-10, Aug. 2013.

[30] K. Hidaka and Y. Murooka, "Electric field measurements in long gap discharge using Pockels device," *IEE Proceedings A*, vol. 132, no. 3, pp. 139–146, May 1985.

[31] R. Zeng, B. Wang, Z. Yu, and W. Chen, "Design and application of an integrated electro-optic sensor for intensive electric field measurement," vol. 18, no. 1, pp. 312–319, Feb. 2011.

[32] R. Zeng, C. Zhuang, Z. Yu, Z. Li, and Y. Geng, "Electric field step in air gap streamer discharges," *Applied Physics Letters*, vol. 99, no. 22, pp. 221503-1–221503-3, Nov. 2011.

[33] R. Zeng, J. Yu, B. Niu, B. Wang, C. Li, H. Wang, and W. Chen, "Integrated optical sensors for wide band time domain electric field measurement," *Proceedings of the CSEE*, vol. 34, no. 29, pp. 5234–5243, Oct. 2014.

Xuan Zhou was born in Yongzhou, Hunan, China, in 1992. She received her B.Eng. degree from the Department of Electrical Engineering, Tsinghua University in Beijing in 2012, where she is currently pursuing a Ph.D. degree. Her research interest is mainly focused on the mechanism and characteristics of long air gap discharge.

She Chen was born in Changsha, Hunan, China, in 1988. He received his B.Eng. and Ph.D. degrees from the Department of Electrical Engineering, Tsinghua University in Beijing in 2010 and 2015, respectively. He is now a lecturer in the Department of Electrical and Information Engineering, Hunan University. His research interest is mainly focused on the theory and characteristics of long air gap discharge.

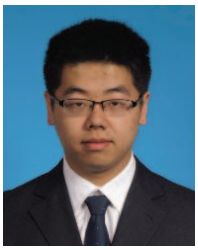

Hai Wang was born Jingzhou, Hubei, China, in 1992. He received his B.Eng. degree from the Department of Electrical Engineering, Tsinghua University in Beijing in 2014, where he is currently pursuing a Ph.D. degree. His research interest is mainly focused on the integrated optical electric field sensors.

Rong Zeng (M'02–SM'06) was born in Shaanxi, China, in 1971. He received the B.Eng., M.Eng., and Ph.D. degrees from the Department of Electrical Engineering, Tsinghua University, Beijing, China, in 1995, 1997, and 1999, respectively. He was a lecturer with the Department of Electrical Engineering, Tsinghua University in 1999, an associate professor and professor with the same department in 2002 and 2007, respectively. Currently, he is the Dean of the Electrical Engineering Department, Tsinghua University. He is currently working in the fields of air gap discharge, lightning protection, and electromagnetic compatibility in power systems, focusing on the hybrid research of electric and magnetic field measurement by integrated electro-optical sensors and numerical simulations of long air gap discharge processes.

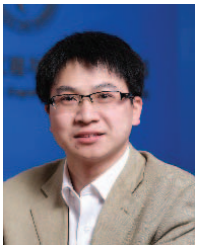

Chijie Zhuang (M'12) was born in Zhejiang, China, in 1983. He received the B.Eng. and Ph.D. degrees from the Department of Electrical Engineering, Tsinghua University, Beijing, China, in 2006 and 2011, respectively. He is currently a Research Assistant with the Department of Electrical Engineering. His current research interests include numerical computation and air gap discharge.

Junjie Yu was born in Zhejiang, China, in 1988. He received his B.Eng. degree from the Department of Electrical Engineering, Tsinghua University in Beijing in 2011, where he is currently pursuing the Ph.D. degree. His research interest is mainly focused on the integrated optical electric field sensors.

Yujian Ding was born in 1982. He received the B.Eng. and M.Eng. degrees from North China Electric Power University, Beijing, China, in 2004 and 2007, respectively. He is currently a Senior Engineer in China Electric Power Research Institute, Beijing, China. His research interests mainly include characteristics of long air gap discharge, external insulation and altitude correction of UHV AC/DC transmission systems, live working on transmission line and insulator detecting.